Eur. Phys. J. D (2025)79:10
https://doi.org/10.1140/epjd/s10053-025-00953-8

THE EUROPEAN PHYSICAL JOURNAL D

Regular Article – Ultraintense and Ultrashort Laser Fields

Two-photon excited fluorescence with shaped laser pulses for refractive beams

S. S. A. S. Bukhari, R. Gottschalk, and A. Lindinger[a]

Institut für Experimentalphysik, Freie Universität Berlin, Arnimallee 14, D-14195 Berlin, Germany

Received 8 October 2024 / Accepted 9 January 2025

Abstract. We report two-photon excited fluorescence of dyes for refracted laser beams by utilizing tailored laser pulses. A fluorescence contrast difference due to phase shaping could be achieved between different coumarin dyes. Particularly, an increased contrast difference is obtained for configurations close to the Brewster angle. Furthermore, by using a subsequent deformable phase plate for spatial shaping it was possible to precisely adjust the laser beam for controlled refraction at the liquid dye surface. A polarization-dependent refraction was observed when directing the shaped laser beam on the curved liquid adhesion meniscus close to the cuvette wall. This results in a refraction-dependent contrast difference. The presented method could be utilized for surface-sensitive biophotonic imaging applications.

1 Introduction

Shaping of ultrashort laser pulses became a topical research tool due to the possibility to control molecular processes [1–4] and various novel applications emerged [5–7]. Recently, also the modification of the polarization state was included in pulse shaping [8,9]. The tailored light fields were particularly employed for multiphoton excited fluorescence, whereby intrapulse interference is utilized to photoexcite differing substances [10]. This is applied for multiphoton excited three-dimensional imaging [11].

In parallel, the spatial modification of laser beam profiles emerged by using two-dimensional modulators and focusing lenses assembled to spatial beam shapers [12]. Two-dimensional phase modifications of liquid crystal modulators result in defined beam profiles in the focal plane, which are applied for beam focusing in tissue [13], microstructuring [14], or high resolved spatial imaging [15]. Currently, spatial and temporal laser pulse shaping was combined in order to spatially and temporally control photo-induced processes. These generated light fields were characterized in first experiments [16–18], but further applications were mainly lacking up to now.

In this contribution, we perform measurements of two-photon excited fluorescence on dyes to investigate refractive laser beams by employing shaped laser pulses. The modification of the fluorescence contrast difference due to phase shaping will be examined between different coumarin dyes for configurations close to the Brewster angle. Moreover, by utilizing a deformable phase plate for spatial shaping the laser beam will precisely be adjusted for different refraction conditions at the liquid dye surface. Polarization-dependent refraction will be investigated by directing the tailored laser beam on the curved liquid adhesion meniscus close to the cuvette wall.

2 Experimental setup

The experiment is presented schematically in Fig. 1. A Nd:YVO_4 laser (Verdi V, Coherent, Inc.) pumps a titanium sapphire laser oscillator (MIRA, Coherent Inc.) which has an average power of 500 mW, a pulse duration of 70 fs, and a repetition rate of 76 MHz. The laser wavelength is at about 800 nm with a full width at half maximum of approximately 30 nm. The laser beam is directed through a 4f-pulse shaper with a computer-controlled liquid crystal light modulator (SLM 640, Cambridge Research Instruments). This enables a modification of the laser pulse phase and polarization. The spectral phase can separately be modulated on the polarization axes at ±45° to the horizontal, respectively. A $\lambda/2$-waveplate is located before the second grating of the shaper in order to rotate the light field by 45° such that the light components modified by the liquid crystals are turned to horizontal and vertical direction, respectively. A polarizer can optionally be placed in the 4-f setup to remove one polarization component.

The laser beam is then guided through a 2D deformable phase plate wavefront modulator (Delta 7,

[a] e-mail: lindin@physik.fu-berlin.de (corresponding author)

Published online: 31 January 2025

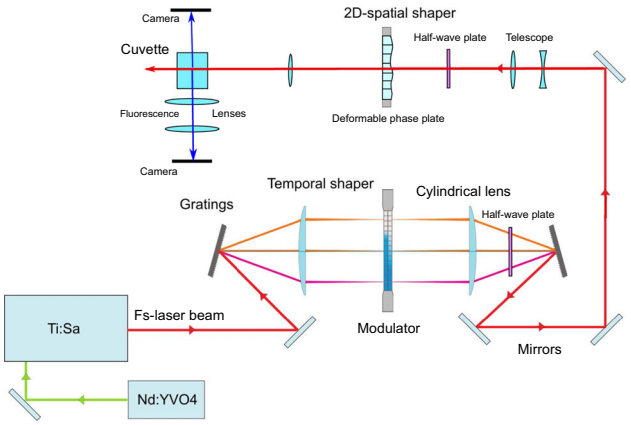

Fig. 1 Experimental setup including a Ti:Sa laser, a temporal laser pulse shaper with gratings and a liquid crystal light modulator, a 2D deformable phase plate modulator, a cuvette, and a fluorescence detection unit. The fs-laser beam passes the temporal pulse shaper, the half-wave plate, the spatial pulse modulator, and is finally focused into cuvettes. The two-photon excited fluorescence is collected by lenses and is guided on a camera

Phaseform GmbH) to generate spatially shaped beam profiles. The deformable phase plate has an electrode array in the active area with a diameter of 10 mm, and it locally changes the optical path length, the geometric length times refractive index, traveled by light. The transmissive device is less than 1 mm thick and consists of a sealed liquid filled volume with a flexible polymeric membrane on one side and a rigid, transparent glass substrate on the other. The volume between the membrane and the substrate is filled with a high-refractive-index liquid. The conductive membrane is pulled toward the substrate when a voltage is applied to the electrodes. This actuation displaces the liquid and changes the effective optical path length of light that refracts through the wavefront modulator. A $\lambda/2$-waveplate is located before the spatial modulator in order to turn the light polarization as required. The polarization properties will not be affected by the spatial modulator, and all polarization components will spatially be shaped equally.

Subsequently, the laser beam is focused in a 2f-setup by a lens (f =150 mm) located 150 mm behind the 2D modulator in order to realize spatially tailored profiles in the focal plane. For the fluorescence experiments, the beam is directed into quartz glass cuvettes filled with the dyes coumarin 102 ($c102$) and coumarin 120 ($c120$) (received from Radiant Dyes) dispersed in highly viscous glycerol. The two-photon excited fluorescence is collected and focused by two convex lenses on a detection camera (C270, Logitech) positioned perpendicular to the beam. A glass filter (BG 39) is used to reduce the stray light of the laser. Another camera (C300, Logitech) is located on the other side of the beam without further lenses in order to directly monitor the fluorescence beam path.

3 Results

The experiments are performed with tailored pulses of refracting laser beams in liquid dye solutions. The first part describes the features for two cuvettes with different incident angles by using temporally shaped laser pulses. A spatial beam shaper is additionally utilized in the second part to precisely direct the laser beam on the adhesive meniscus of the liquid dye solution in order to conduct surface-sensitive refraction studies. These measurements are particularly conducted in order to modify and enhance the fluorescence contrast difference between the coumarin dyes.

3.1 Two-photon fluorescence depending on the polarization of the exciting laser beam

In these measurements, the focused laser beam first passes a cuvette filled with coumarin 120 dispersed in glycerol and then another cuvette filled with coumarin 102 in glycerol. The second cuvette is thereby turned by an azimuthal angle of about 56°, i.e., close to the Brewster angle (see left inset of Fig. 2). With this geometry, it is feasible to compare normal incidence and Brewster angle tilted incidence. Polarization-dependent experiments are performed by rotating the waveplate before the cuvettes, and the two-photon excited fluorescence is recorded perpendicular to the beam direction (see the experimental setup in Fig. 1).

The two-photon excited fluorescence is received by adding up the signals of the camera pixels for the corresponding luminescent region of each dye.

In Fig. 2, the polarization-dependent fluorescence intensities from short pulses are depicted for both dyes, respectively. Connecting lines are shown for better visibility. A strong signal oscillation can be observed for the two-photon excited fluorescence of coumarin 120 at normal angle incidence with a maximum for vertical and a minimum for horizontal polarization direction. This can be explained by the dipole fluorescence emission characteristics of the molecules in high viscous glycerol. After photoexcitation, the molecule is barely able to rotate away until it fluoresces. Hence, for vertically polarized excitation the detector records the strong emission perpendicular to the dipole, whereas for horizontal polarization only the weak emission in dipole direction can be observed. The inset on the right side shows the results of coumarin 102 at normal incidence for comparison. The small differences between the two dyes at normal incidence are probably due to the slightly differing anisotropy properties.

For coumarin 102 at Brewster angle incidence, the intensity amplitude is considerably reduced. This can mainly be attributed to the effect of the irradiation close to the Brewster angle. For horizontally polarized pulses, the transmission of the beam into the rotated cuvette is almost undiminished, whereas for vertical polarization it is more reduced. This effect is enlarged in the present experiment because the two-photon excited fluorescence has a quadratic signal dependence on the

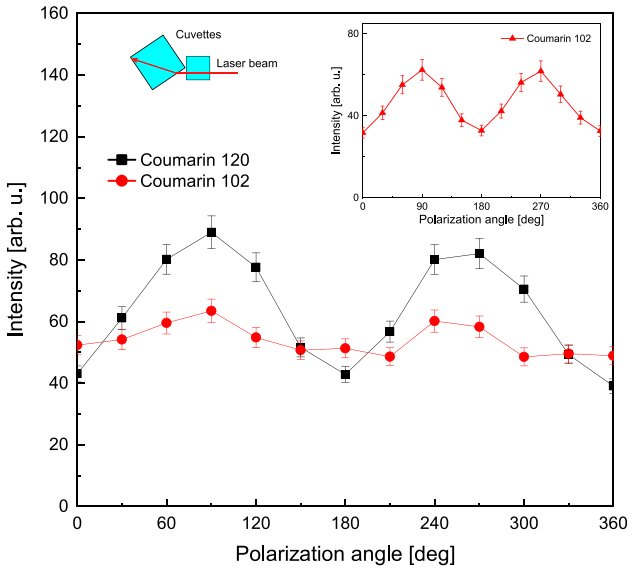

Fig. 2 Polarization-dependent two-photon excited fluorescence intensities from short pulses for one cuvette in normal and another in Brewster angle configuration. A large signal oscillation is obtained for the fluorescence of coumarin 120 from the first cuvette at normal incidence, with a maximum for vertical and a minimum for horizontal polarization direction. For the second cuvette, filled with coumarin 102, the intensity amplitude is considerably reduced which is mainly due to the effect of the irradiation close to the Brewster angle. The inset on the left shows a top-view scheme of one cuvette at normal incidence and the other at Brewster angle incidence, and the inset on the right shows the results of coumarin 102 at normal incidence for comparison

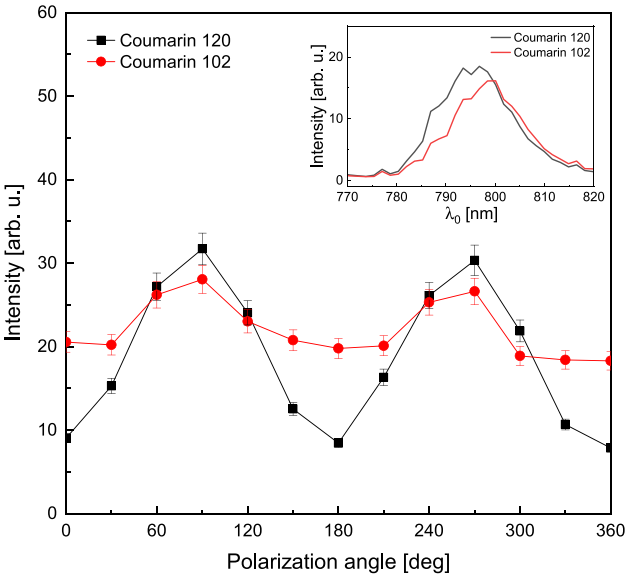

Fig. 3 Polarization-dependent fluorescence intensities for the two dyes with the phase center wavelength at $\lambda_0 = 808$ nm. Upshifted data are observed for coumarin 102 compared to coumarin 120 with respect to a short pulse. This can be attributed to the relatively larger fluorescence at the red-shifted phase center wavelength compared to a short pulse. The inset shows the two-photon excited fluorescence intensities by tuning the phase center wavelength for the two coumarin dyes

irradiating laser light intensity. In the following, it will be explained how this feature is utilized to modify the fluorescence contrast between the two dyes.

In order to control the two-photon excited fluorescence, tailored laser pulses are produced by inscribing antisymmetric phase functions $\phi(\omega) = \frac{b_3}{6}(\omega - \omega_0)^3$ on a liquid crystal array of the temporal pulse shaper, having a third-order phase factor $b_3 = 2 \cdot 10^5$ fs^3 with differently tuned phase center frequencies ω_0. This permits frequency selective two-photon excitations with sharp maxima due to constructive interference at the corresponding phase center frequencies [10]. With these antisymmetric third-order phase functions, it is hence possible to conduct frequency selective excitation by shifting the antisymmetric phase center which leads to a contrast difference. The value of the phase factor was chosen to receive clearly differing scan results. A polarizer adjusted at an angle of 45° to the horizontal is placed in the temporal pulse shaper in order to ensure purely linear polarization.

The inset of Fig. 3 displays the two-photon excited fluorescence intensities by tuning the phase center wavelength $\lambda_0 = 2\pi c/\omega_0$ for the two coumarin dyes. A red-shift of the spectrum for coumarin 102 relative to the spectrum of coumarin 120 can be observed which leads to a distinct contrast difference for the two dyes. The polarization-dependent fluorescence intensities for the two dyes are presented in Fig. 3 where the phase center wavelength is adjusted to $\lambda_0 = 808$ nm. An upshift of the data for coumarin 102 relative to coumarin 120 compared to the results for a short pulse (see Fig. 2) is obtained. This can be explained by the relatively higher fluorescence signal at this red-shifted phase center wavelength compared to a short pulse.

These features are utilized to investigate the modification of the fluorescence contrast $c = (I_{c102} - I_{c120})/(I_{c102} + I_{c120})$ between the two coumarin dyes. Figure 4 presents the contrasts of coumarin 120 in the first and coumarin 102 in the second cuvette at different polarization directions for parallel in-line cuvettes (a) and for a first parallel and a second Brewster angle turned cuvette (b). It can be observed that the contrast values for the phase-shaped pulses are in both cases higher than the contrast values for short pulses which is due to the higher signal of coumarin 102 for the red-shifted two-photon excitation. Considerably larger signal modulations with higher maxima are obtained for the Brewster angle configuration. This can be explained by the additional effect of the polarization-dependent transmission. For short pulses, only the effect of the Brewster angle will be observed as visible in Fig. 4 (black lines), and for shaped pulses the spectral and the Brewster angle effect is responsible (blue lines). Hence, the maximal contrast difference rises from about $\Delta c = 0.1$ for short pulses with parallel in-line cuvettes to about $\Delta c = 0.4$ for the phase-shaped pulses in Brewster

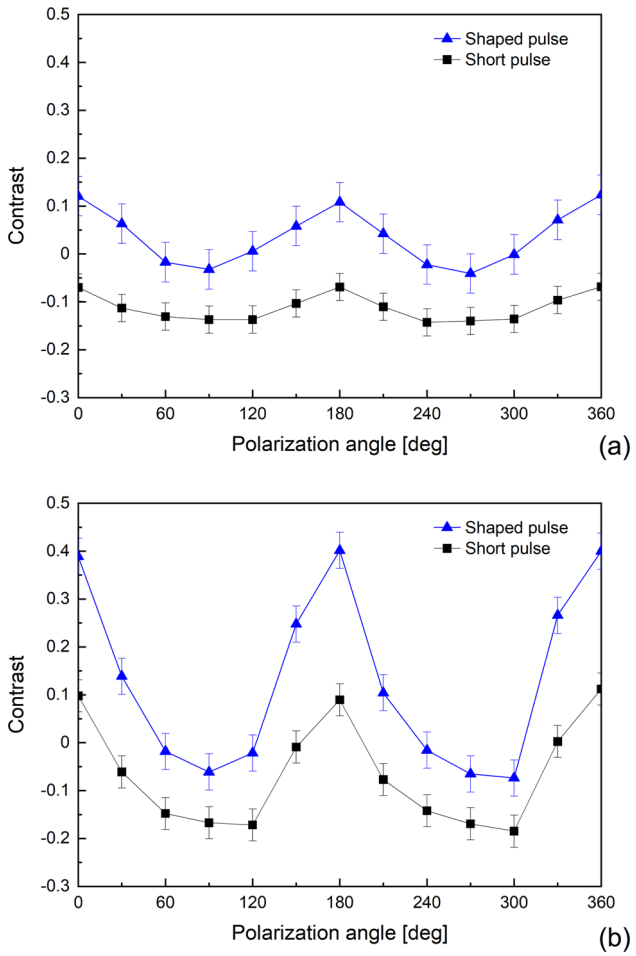

Fig. 4 Contrasts of the two dyes at different polarization directions for cuvettes in parallel in-line (a) and Brewster angle (b) configuration, respectively. The contrast values for the phase-shaped pulses are in both cases higher than the contrast values for short pulses which is attributed to the higher signal of coumarin 102 for the red-shifted two-photon excitation. Considerably larger signal modulations with higher maxima are obtained for the Brewster angle configuration (b) which is due to the polarization-dependent transmission. Therefore, the maximal contrast difference rises from short pulses with in-line cuvettes to phase-shaped pulses with cuvettes in Brewster geometry

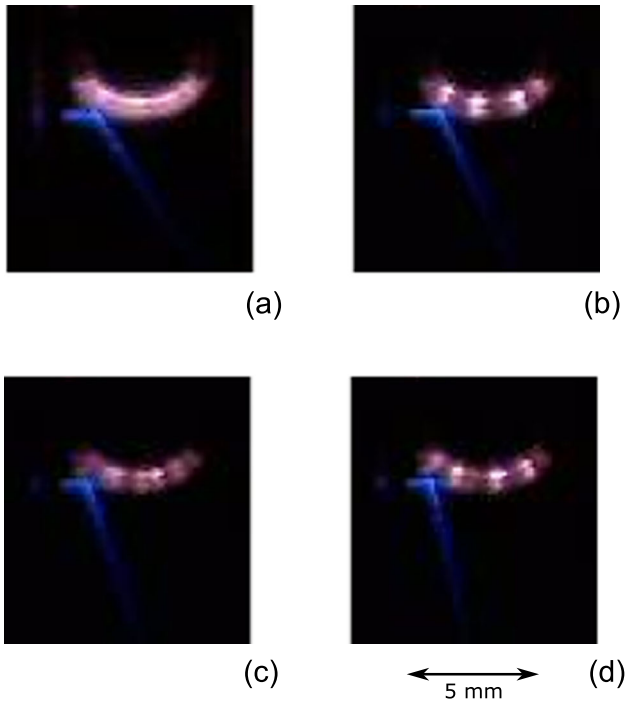

Fig. 5 Images of the fluorescence due to vertically changed beam paths by a perpendicularly positioned camera. For these low beam positions, the beam is reflected from the curved meniscus and propagates downwards. An image sequence is displayed for the prefactors -5 (a), -2 (b), 1 (c), and 4 (d) of the Zernike polynomial Z_1^{-1}. This corresponds to slightly increasing beam heights of 90 μm (b), 180 μm (c), and 270 μm (d) where the reflected beam propagates at further downward angles

geometry. The contrast difference can even be increased by comparing blue shifted two-photon excitation pulses for vertical polarization with red-shifted two-photon excitation pulses for horizontal polarization.

3.2 Surface sensitive refraction for enhanced two-photon excited fluorescence contrasts

The curved shapes of liquid surfaces are of interest, e.g., in liquid–solid contact ranges, meniscuses, or oscillating surfaces. They can be investigated by laser irradiation into the meniscus to receive its shape by reflection [22], to measure the liquid–solid contact angle [23], and to study meniscus oscillations [24]. Furthermore, novel applications of shaped liquid surfaces like laser beam steering [25] came up. Here we direct the laser beam on the meniscus close to the cuvette wall and investigate the polarization-dependent refraction which leads to differing two-photon excited fluorescence. For this experiment, the deformable phase plate for spatial shaping will additionally be used and the lens before the cuvette will be replaced by a lens with f = 100 mm to ensure better focusing conditions. After the spatial shaper, the horizontally propagating laser beam will be focused to positions near the upper liquid dye surface (coumarin 120). The tailored beam will pass the cuvette wall with the adherent liquid and is then directed on the curved liquid adhesion meniscus close to the cuvette wall. By utilizing the spatial modulator, the beam height is slightly changed that it hits at different heights on the curved adhesion meniscus. This is performed by inscribing the Zernike polynomial Z_1^{-1} with differing prefactors on the spatial modulator. In the present optical setup, a step of 1 in the prefactor corresponds to a step of only about 30 μm in beam height at the position of the cuvette which demonstrates the high precision of the spatial modulator.

Figure 5 presents images of the modified beam paths and the induced fluorescence recorded with the perpen-

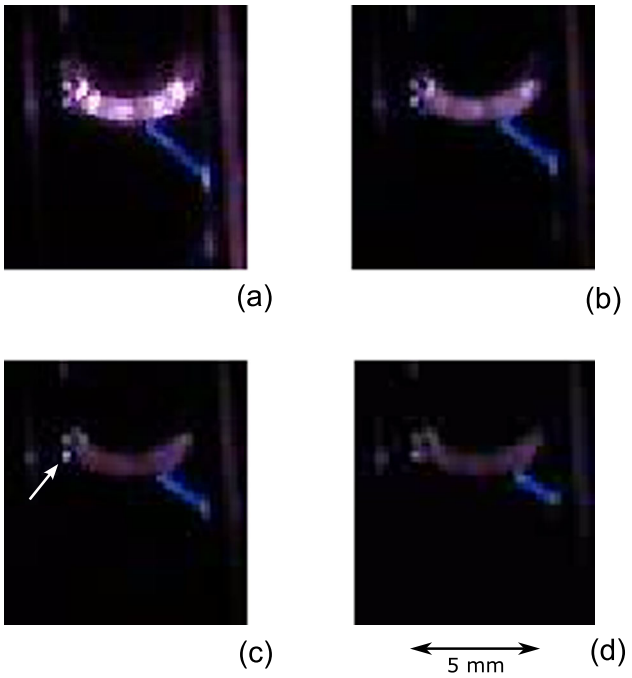

Fig. 6 Images of the fluorescence at a higher beam position with vertically modified beam paths recorded by a perpendicularly positioned camera. Images are shown for the prefactors -5 (a), -2 (b), 1 (c) and 4 (d) of the Zernike polynomial Z_1^{-1} corresponding to incrementally enhanced beam heights of 90 μm (b), 180 μm (c), and 270 μm (d). Here the beam is refracted back to air, and at a position on the other side of the cuvette it is refracted back into the liquid and propagates down at a certain angle. The point of refraction back into the liquid moves further away and the refraction angle gets smaller for higher beam positions

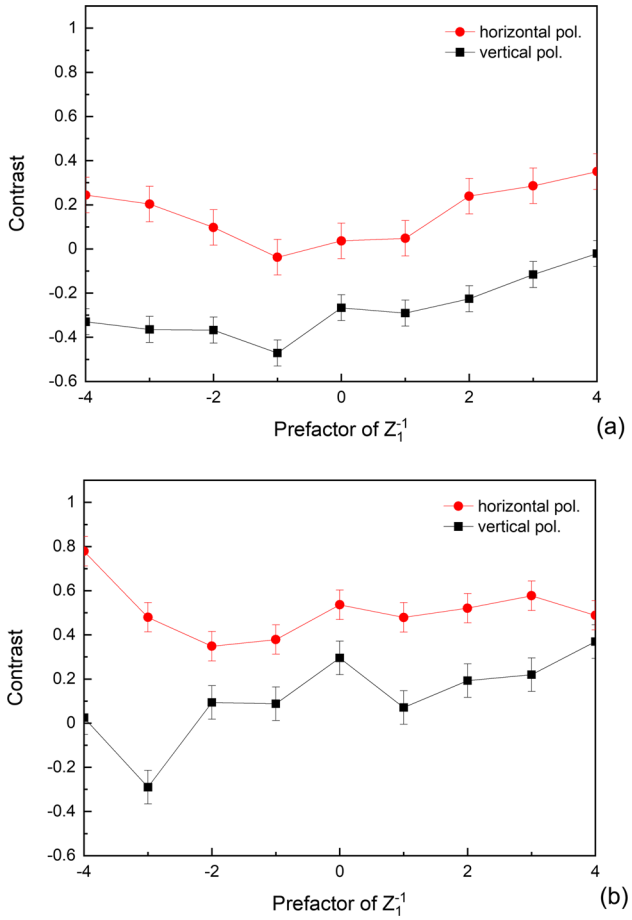

Fig. 7 Fluorescence contrast signals for the normal directed beam in coumarin 102 and the refracted beam in coumarin 120 are plotted for different prefactors of the Zernike polynomial Z_1^{-1} corresponding to different beam heights. The horizontal and vertical polarization contrasts for the phase center wavelength $\lambda_0 = 792$ nm are presented in (a), and the horizontal and vertical polarization for $\lambda_0 = 806$ nm in (b)

dicularly positioned camera without lenses and infrared filter. It can be observed that for low beam positions the beam is reflected from the curved meniscus such that it propagates downwards. An image sequence is displayed for incrementally increasing beam positions where the reflected beam is propagating at more downward directed angles.

For even higher beam positions, shown in Fig. 6, the beam is refracted back to air at the curved meniscus close to the entrance wall, and at a position on the other side of the cuvette it is refracted again into the liquid such that it propagates down at a certain angle. This angle gets smaller for higher beam positions, and the point of refraction back into the liquid moves further away to the other side of the cuvette. For these higher beam positions, a small spot at the entrance wall close to the curved meniscus is visible, marked by an arrow in Fig. 6(c).

These differing paths can be explained by the curved liquid adhesion surface, because at lower beam positions the incidence angle to the surface normal is larger than the total reflection angle which leads to reflection, whereas for higher positions the angle is smaller than the total reflection angle leading to refraction into air. By additionally applying the Zernike polynominal Z_2^0 with corresponding prefactors, it is further possible to shift the focus in beam direction such that the fluorescence is stronger at different positions. These features demonstrate the precision of the deformable phase plate. Single adjustments like beam positioning could also be done with high-precision mounts but the modulator enables fast and flexible modulations, and furthermore, simultaneous beam shaping can be performed like different focusing depths or flexible astigmatic shaping, vortex beams, and higher beam corrections. This could be conducted in further perspective studies.

Polarization-dependent refraction is investigated by rotating the half-wave plate before the cuvette for different beam heights. The fluorescence is collected by two lenses and directed on the camera, as depicted in Fig. 1. The signals from the separately fluorescing ranges of the two cuvettes were simultaneously recorded for each dye. The refracted beam signals for vertical

polarization are generally higher than for horizontal polarization due to the above described dipole effect. Yet, the signals of the refracted beam are even further enhanced which can be attributed to the two refractions at angles not too far from be Brewster angle. Thus, the vertically polarized beams transmit only with minor intensity reduction, whereas the horizontally polarized beam intensities are considerably reduced. The visibility of this effect is even increased for the two-photon excited fluorescence because it has a quadratic intensity dependence. For spatial shaping by phase modulation, only little change of the light intensities and hence of the two-photon excited fluorescence signal is expected for low prefactors of the Zernike polynomial Z_1^{-1} (as visible in Figs. 5 and 6), and the recorded contrast values do not depend on the light intensities due to the intensity ratio in the contrast formula.

In Fig. 7, the two-photon excited fluorescence contrast between coumarin 102 for the normal beam and coumarin 120 for the refracted beam direction is plotted for different prefactors of the Zernike polynomial Z_1^{-1} corresponding to different beam heights. Figure 7(a) shows the horizontal and vertical polarization contrasts for the phase center wavelength $\lambda_0 = 792$ nm and Fig. 7(b) for $\lambda_0 = 806$ nm. It can be observed that the contrast for the larger phase center wavelength from (b) is generally higher than the smaller phase center wavelength contrasts from (a) which can be explained by the relatively higher fluorescence of coumarin 102 compared to coumarin 120 at larger excitation wavelengths. Moreover, the contrasts for horizontal polarization are in both cases larger than the contrasts for vertical polarization. This is due to the diminished light reduction for the refractions near the Brewster angle in vertical polarization direction. Hence, the coumarin 120 fluorescence is larger for vertical than for horizontal polarization, and therefore, the contrasts are larger for horizontal than for vertical polarization. An increased maximal contrast difference of about $\Delta c = 0.6$ between horizontal polarization from (a) and vertical polarization from (b) can be achieved by utilizing both effects, the wavelength-dependent excitation and the Brewster angle refraction.

It is shown that contrast difference enhancement by using a Brewster angle configuration can be performed on the micrometer-scale size of a curved liquid from a meniscus. The effect of the Brewster angle is visible in Fig. 7 by comparing black (with Brewster effect) and red lines (no Brewster effect). The other enhancement effect originates from the two different phase center wavelengths with higher contrast values in Fig. 7(b) than in (a) due to the higher signals of coumarin 102 compared to coumarin 120 at higher wavelengths. Both effects together lead to the increased contrast difference. Hence, even at this small scale and with having not exactly the Brewster angle it is possible to achieve a contrast enhancement effect.

4 Conclusion

Two-photon excited fluorescence of coumarin dyes has been investigated for refracted laser beams by employing shaped laser pulses. Fluorescence contrasts were obtained by pulse shaping with appropriate third-order phase functions, and an enlarged contrast difference was achieved for beam geometries with one cuvette at normal incidence and another at close to Brewster angle incidence. In a second experiment, a deformable phase plate was additionally inserted for spatial shaping. This enabled an exact adjustment of the laser beam for controlled reflection or refraction at the liquid dye surface. Particularly, a polarization-dependent refraction could be obtained by directing the tailored laser beam on the curved liquid adhesion meniscus near the cuvette wall which leads to a refraction-enhanced contrast difference. The first experiment can be regarded as a demonstration of the contrast enhancement by using a Brewster angle configuration. It shows that the contrast difference can be increased in this geometry. In the second experiment, this effect is applied on the micrometer-scale size of a curved liquid from a meniscus. Even at this small scale and with having not exactly the Brewster angle, it is possible to achieve the contrast enhancement effect. The presented method has a high potential for liquid surface biophotonic applications.

Acknowledgements The authors thank Prof. Dr. W. Kuch and the team of Phaseform GmbH for supporting this experimental study.

Author contributions

SSASB conducted the experiment, analyzed the results, and refined the manuscript. RG computed the data acquisition and refined the manuscript. AL conceived and supervised the project, performed the experiment, and wrote the manuscript.

Data Availability Statement This manuscript has no associated data or the data will not be deposited. [Authors' comment: Data will be made available on reasonable request.]

References

1. T. Brixner, G. Gerber, Chem. Phys. Chem. **4**, 418 (2003)
2. R.S. Judson, H. Rabitz, Phys. Rev. Lett. **68**, 1500 (1992)
3. P. Nuernberger, G. Vogt, T. Brixner, G. Gerber, Phys. Chem. Chem. Phys. **9**, 2470 (2007)
4. A. Assion, T. Baumert, M. Bergt, T. Brixner, B. Kiefer, V. Seyfried, M. Strehle, G. Gerber, Science **282**, 919 (1998)
5. W. Wohlleben, T. Buckup, J.L. Herek, M. Motzkus, Chem. Phys. Chem. **6**, 850 (2005)
6. M. Aeschlimann, M. Bauer, D. Bayer, T. Brixner, F.J. Garcia de Abajo, W. Pfeiffer, M. Rohmer, C. Spindler, F. Steeb, Nature **446**, 301 (2007)
7. A. Lindinger, C. Lupulescu, M. Plewicki, F. Vetter, A. Merli, S.M. Weber, L. Wöste, Phys. Rev. Lett. **93**, 033001 (2004)
8. L. Polachek, D. Oron, Y. Silberberg, Opt. Lett. **31**, 631 (2006)
9. F. Weise, A. Lindinger, Appl. Phys. B **101**, 79 (2010)
10. V.V. Lozovoy, I. Pastirk, K.A. Walowicz, M. Dantus, J. Chem. Phys. **118**, 3187 (2002)
11. W. Denk, J.H. Strickler, W.W. Webb, Science **248**, 73 (1990)
12. C. Maurer, A. Jesacher, S. Bernet, M. Ritsch-Marte, Laser. Photonics. Rev. **5**, 81 (2011)
13. A. Tanabe, T. Hibi, S. Ipponjima, K. Matsumoto, M. Yokoyama, M. Kurihara, N. Hashimoto, T. Nemoto, J. Biomed. Opt. **20**, 101204 (2015)
14. N. Sanner, N. Huot, E. Audouard, C. Larat, J.P. Huignard, Opt. Lasers Eng. **45**, 737 (2007)
15. G. Moneron, S. Hell, Opt. Exp. **17**, 14567 (2009)
16. D.J. McCabe, A. Tajalli, D.R. Austin, P. Bondareff, I.A. Walmsley, S. Gigan, B. Chatel, Nature Commun **2**, 447 (2011)
17. T. Feurer, J.C. Vaughan, R.M. Koehl, K.A. Nelson, Opt. Lett. **27**, 652 (2002)
18. T. Feurer, J.C. Vaughan, K.A. Nelson, Science **299**, 374 (2003)
19. M.J. Snare, F. Treloar, K.P. Ghiggino, P.J. Thistlethwaite, J. Photochem. **18**, 335 (1982)
20. R.F. Kubin, A.N. Fletcher, J. Luminescence **27**, 455 (1982)
21. T. Wu, J. Tang, B. Hajj, M. Cui, Opt. Express **19**, 12961 (2011)
22. A.J.J. van der Zanden, A.K. Chesters, Int. J. of Multiphase Flow **20**, 775 (1994)
23. T.F. Eibach, D. Fell, H. Nguyen, H.J. Butt, G.K. Auernhammer, Rev. Sci. Instrum. **85**, 019703 (2014)
24. R.H. Farahi, A. Passian, Y.K. Jones, L. Tetard, A.L. Lereu, T.G. Thundat, Opt. Lett. **34**, 3148 (2009)
25. Y. Cheng, J. Cao, Q. Hao, Opt. Laser. Eng. **146**, 106700 (2021)